Journal of Pineal Research

WILEY

Journal of Pineal Research
Molecular, Biological, Physiological and Clinical Aspects of Melatonin

ORIGINAL ARTICLE OPEN ACCESS

Melatonin Prevents Tumor Growth: The Role of Genes Controlling the Circadian Clock, the Cell Cycle, and Angiogenesis

Skarleth Cardenas-Romero[1] | Nadia Saderi[1] | Oscar Daniel Ramirez-Plascencia[1] | Adrián Baez-Ruiz[1] | Omar Flores-Sandoval[1] | Carolina Escobar Briones[2] | Roberto C. Salgado-Delgado[1]

[1]Laboratorio de Neuroanatomía Funcional y Ritmos Biológicos, Facultad de Ciencias, Universidad Autónoma de San Luis Potosí, San Luis Potosí, México | [2]Laboratorio de Ritmos Biológicos y Metabolismo, Facultad de Medicina, Departamento de Anatomía, Universidad Nacional Autónoma de México, México City, México

Correspondence: Roberto C. Salgado-Delgado (roberto.salgado@uaslp.mx)

Received: 28 February 2025 | **Revised:** 2 June 2025 | **Accepted:** 5 June 2025

Funding: This study was supported by Consejo Nacional de Ciencia y Tecnología.

Keywords: angiogenesis | cell cycle | circadian rhythm | clock genes | glioblastoma | melatonin

ABSTRACT

Recent evidence highlights the protective role of melatonin in a variety of pathological conditions, including multiple types of cancer. Epidemiological studies increasingly suggest that exposure to light at night suppresses melatonin synthesis in night-shift and rotating-shift workers, potentially elevating their risk of cancer development. Experimental data further indicate that melatonin can inhibit the proliferation of tumor cells, including glioblastoma-like stem cells. In the present study, we investigated the effect of melatonin on the expression of genes involved in regulating the circadian rhythm, cell cycle progression, and angiogenesis in rats exposed to constant light, a model of circadian disruption. Our findings demonstrate that melatonin administration significantly inhibited tumor growth and reduced the vascularization associated with circadian rhythm disturbance. Molecular analysis revealed that melatonin altered the circadian expression of several genes affecting tumor biology, including *p53, TNF-α*, *Per2*, *VEGF-A*, *PDGF-C*, and *Ang*, which are involved in circadian rhythms, cell cycle, and angiogenesis regulation. These results strengthen the existing hypothesis that circadian disruption contributes to tumor progression and suggest that melatonin exerts anticancer effects by modulating circadian gene expression and angiogenesis. Our findings provide further insight into the mechanism by which melatonin may exert oncostatic effects and highlight its potential as a therapeutic agent in cancers associated with circadian rhythm disruption.

1 | Introduction

Evolution has equipped organisms with a biological clock (the suprachiasmatic nucleus; SCN) to help them anticipate and adapt to daily environmental changes, thereby enhancing their chances of survival. The biological clock gets synchronized by external time cues, known as Zeitgebers, such as the light–dark cycle. However, the desynchronization between the biological clock and the environment can undermine cellular health and has been shown to trigger or worsen several pathological conditions.

The circadian misalignment caused by nighttime exposure to light in shift workers, like animal models of circadian desynchronization, has been shown to suppress the daily peak of melatonin production at the beginning of the night, which is associated with an increased risk of tumorigenesis [1, 2].

Melatonin is an internal synchronizer with pleiotropic effects on the central and peripheral regulation of circadian rhythms, as well as on cell proliferation, adhesion, apoptosis, angiogenesis, and inflammation [3, 4]. At night, the SCN stimulates the pineal gland to synthesize and secrete melatonin, signaling through the G-protein-coupled receptors MT1R and MT2R [5].

Over the last few years, several pieces of evidence have suggested that preserving the circadian rhythms of body physiology and behavior, as well as adjusting anticancer therapy to the daily patterns of the host, could play a protective role in the onset and progression of Glioblastoma (GBM) [6–10]. The GBM is the most common malignant brain tumor, representing nearly 54% of all diagnosed gliomas, and, in most cases, it tends to recur after chemotherapy and radiotherapy [11].

In this study, we investigated whether the protective and antitumoral properties of melatonin are associated with its capacity to modulate the molecular circadian clock. Specifically, we analyzed the circadian expression of genes involved in circadian regulation (*Per2*, *Bmal1*, *Rorα*, and *Rev-erbα*), cell cycle control (*p53*, *p21*, and *cyclin E*), and angiogenesis (*VEGF-A*, *PDGF-C*, *TNF-α*, and *Ang*) in both GMB tissue and the liver of rats exposed to either a standard light-dark cycle or constant light to induce circadian disruption. Our results showed that melatonin administration restored circadian rhythmicity and significantly inhibited tumor growth, as well as reduced vascularization within GBM tissue induced by constant light exposure. Furthermore, melatonin altered the circadian expression patterns of key genes: In GBM tissue, *p53* and *TNF-α* were modulated, while in the liver, changes were observed in *Per 2*, *cyclin E*, *VEGF-A*, *PDGF-C*, *TNF-α*, *Ang*, and *MT1R*. Additionally, melatonin influenced the overall 24-h expression levels of several genes in GBM tissue (*Per2*, *Rorα*, *p53, VEGF-A*, *PDGF-C*, *TNF-α*, and *Ang*) and the liver *(Per2*, *Rorα*, *Rev-erbα*, *p21*, *Cyclin E, VEGF-A*, *PDGF-C*, *TNF-α*, and *Ang*) compared to synchronized control rats. Taken together, these findings suggest that the circadian modulation of plasma melatonin exerts a protective effect on cellular physiology and contributes to the attenuation of GBM aggressiveness, even under conditions of circadian desynchronization.

2 | Materials and Methods

2.1 | Ethical Approval

All experimental procedures were conducted in accordance by the ethical guidelines established by the Ethics Committee of the Department of Chemical Science (Facultad de Ciencias Químicas) at the Universidad Autonoma de San Luis Potosí (CEID-FCQ, protocol number CEID2014030). The study adhered strictly to the Mexican Official Standard Guidance for the Care and Use of Experimental Animals (NOM-062-ZOO-1999) and followed the European Convention for the Protection of Vertebrate Animals Used for Experimental and Other Scientific Purposes (Council of Europe No.123, Strasbourg 1985).

2.2 | Animals and Experimental Conditions

Male Wistar rats (RRID: RGD_13508588), weighing between 180 and 200 g, were obtained from the Laboratory of Biological Rhythms and Metabolism of Universidad Autonoma de México. Animals were housed individually in transparent acrylic cages within soundproof racks. They were maintained under a controlled 12:12-h light-dark (LD) cycle (lights on at 7:00, off at 19:00; light intensity ~350–370 lux), with controlled temperature (23°C ± 1), continuous airflow, and ad libitum access to filtered water and standard rodent chow (Laboratory Rodent Chow 5001, LabDiet).

Following a 4-day acclimatization period, rats underwent abdominal surgery to implant a sterilized temperature sensor (iButton Maxim integrated™) beneath the peritoneum. The abdominal muscle and skin layers were closed using black braided silk sutures (Atramat™). After 3-day recovery, animals were randomly divided into six experimental groups: LD (12-h light/12-h dark cycle), LL (constant 24-h light), LD-GBM, LL-GBM, LL-GBM-mel (melatonin treatment), and LL-GBM-veh (vehicle administration).

On day 10, LD-GMB, LL-GMB, LL-GMB-mel, and LL-GMB-Veh groups were inoculated in the interscapular region with 8×10^6 C6 glioma cells suspended in 300 μL of RPMI-1640 medium. The LD and LL groups received 300 μL of medium only. Starting on day 17 and continuing until the end of the protocol, the LL-GBM-mel group received melatonin (1.5 mg/kg body weight; Sigma-Aldrich), and LL-GBM-veh received a 3.5% ethanol-water solution once daily at the onset of the subjective night, administered via orogastric gavage. Melatonin was dissolved in 50 mL of a 3.5% ethanol-water solution (Supporting Information S1: Figure 1; Created in BioRender. Cardenas Romero, S. (2025) https://BioRender.com/0cm0fvs).

2.3 | Locomotor Activity and Body Temperature Monitoring

General locomotor activity was recorded using pressure and infrared sensors placed beneath and above the cages as previously described [12]. Behavioral data were collected through a digitalized system, recorded at 1-min intervals, and analyzed using PC SPAD9 software (version 1.1.2, Omnialva SA de CV). Double-plotted actograms were generated for each animal, representing the sum of activity per 15-min interval throughout the experimental period.

Core body temperature was measured every 20 min using programmed sensors to monitor daily temperature rhythms until euthanasia.

2.4 | Tissue Collection

Twenty-eight days after being assigned the animals of the experimental protocols, rats were euthanized at four temporal points (0, 6, 12, and 18 h after lights-on). Rats from LL, LL-GBM, and LL-GBM-mel groups were paired with LD and LD-GBM ($n = 3$–6 per time point). Rats were deeply anesthetized with an overdose of sodium pentobarbital (65 mg/mL; Sedalpharma, Pet's Pharma), and tumors along with the left hepatic lobe were excised and weighed. Approximately half of the tumor and liver tissue were flash-frozen at −80°C. Blood

samples (240 ± 10 μL) were collected at each temporal point in Eppendorf tubes (1.5 mL) containing a clot-activator gel and were centrifuged at 2500 rpm for 10 min. The resulting plasma was stored in aliquots of 80 μL at −80°C until assay. We did not collect tissue from LL-GBM-veh animals.

Subsequently, animals were transcardially perfused with 0.9% saline followed by 4% paraformaldehyde (PFA; Sigma-Aldrich Corp.) in phosphate buffer (PB, 0.1 M, pH 7.4). The remaining tumor tissue was post-fixed in 4% PFA for 24 h, then cryoprotected in a solution of 30% sucrose and 0.04% NaN_3 (Amresco LLC) in phosphate buffer saline (PBS 0.1 M, pH 7.4) at 4°C until processing.

2.5 | Cell Culture and Tumor Inoculation

Glioma C6 cell line (CLS Cat# 500142/p672_C6; RRID: CVCL_0194) was cultured as a monolayer in RPMI 1640 medium (GIBCO) supplemented with 10% fetal bovine serum (GIBCO), under standard conditions (37°C, 5% CO_2, 95% humidity). Cells were washed with Hank's solution (GIBCO) and harvested at 90%–95% confluence in not-supplemented RPMI 1640. Cell quantification was determined using a Neubauer chamber, applying the formula:

$$\text{Total cells} = (\text{Cells counted} \times \text{Chamber volume} \times \text{Dilution factor}/\text{Total volume}.$$

Given the similar growth rate of C6 cells in the brain and subcutaneous tissue, rats were hypodermically inoculated with 8×10^6 cells between the shoulder blades. Tumor growth was monitored using Vernier calipers every 2 days from Day 22 onward. The volume was calculated using the formula: $V = \pi/6$* {(Large Diameter) *(Short Diameter)^2}.

2.6 | Histology and ELISA

Post-fixed GBM tissues were processed in histological cassettes, dehydrated in graded ethanol solutions, embedded in paraffin, and sectioned into 4–5 μm slices. Sections were mounted on gelatin-coated slides, deparaffinized at 64°C for 15 min, and rehydrated with a graded series of alcohols (xylene, ethanol 100%, 90%, 70%) and distilled water. Slides were stained with Mayer´s hematoxylin and eosin (H&E), then cover-slipped. Images were captured using a Leica DM500 light microscope at 10× and 40× magnifications, using Leica Suite Software (version 3.0; FFTW, RRID: SCR_016555).

Melatonin was determined in 25 μL of plasma with a commercial kit (Melatonin ELISA kit; Aviva Systems Biology) as described in the data sheet protocol.

2.7 | Semi-Quantitative RT-PCR

Total RNA was extracted from liver and tumor tissues using Trizol Reagent (Invitrogen) following the manufacturer's instructions. Equal RNA amounts from at least three rats per time point were used to generate complementary DNA. For RT-PCR analysis of clock genes (*Per2*, *Bmal1*, *Rorα*, *Rev-erbα*) and cell cycle genes (*p53*, *p21*, *cyclin E*), 500 ng/μL of RNA per sample was used. For proangiogenic genes (*VEGF-A*, *PDGF-C*, *TNF-α*, *Ang*) and melatonin receptors (*MTR1*, *MTR2*), 250 ng/μL per sample was used. Primer sequences are listed in Supporting Information S6: Table 1. All data were normalized against *GAPDH* expression, and mRNA quantification was performed using ImageJ (RRID: SCR_003070).

2.8 | Data Analysis

Tumor growth over time was analyzed using repeated-measures MANOVA (RM-MANOVA; 95% CI) [13], evaluating time, group, and time × group interactions. Additional RM-MANOVAs were run within each group to assess the time effects independently. All dependent variables were modeled using fixed-linear models (one-way and two-way ANOVA). Model selection was based on the highest R^2 (determination coefficient = explained variation), lowest Akaike Information Criterion (AIC) [14], and the parsimony principle. Model residuals were tested for normality (Shapiro–Wilk test) and homogeneity of variances (Brown–Forsythe test) [15], confirming parametric assumptions. Significant time-point differences were determined by Tukey's post hoc test. Comparisons between non-GBM-bearing groups were made using unpaired Student's *t*-tests and Tukey tests, while comparisons among GBM-bearing groups used Tukey tests. An alpha level of 0.05 was considered significant. Statistical analysis was performed using JMP Pro v10 (SAS Institute Inc., Cary, NC, 1989–2021), and graphs were generated using GraphPad Prism (RRID: SCR_002798). Results are expressed as mean ± standard error.

3 | Results

3.1 | Melatonin Enhances the Circadian Rhythm of Locomotor Activity in Desynchronized Rats

The locomotor activity and core body temperature were registered to bear out constant light's desynchronizing effect and explore melatonin's entraining properties. LD and LD-GBM rats displayed a clear day-night pattern with high locomotor activity and core body temperature during the dark phase (representative actograms in Figure 1A,G), (Day vs. Night mean temperature: $p = 0.0001$ and $p = 0.0058$, respectively; Figure 2A,E). Both groups exhibited rhythmic locomotor activity, where nocturnal activity was 73.784% and 63.288% of the total daily activity (Day vs. Night activity: $p = 0.0001$ and $p = 0.0003$; Figure 1B,H) and body temperature (Figure 2B,F). The visual inspection of actograms and the periodogram indicated that circadian rhythmicity was lost in LL (Figures 1D,E and 2C,D) and LL-GBM rats (Figures 1J,K and 2G,H). Consistent results in LL-GBM-veh were observed (Figures 1P,Q and 2K,L), confirming that the experimental manipulation does not impose an artificial rhythm on the animals. Furthermore, melatonin supplied to constant light-desynchronized rats (LL-GBM-mel) elicited a peak in locomotor activity associated with the time of administration, resulting in a significant difference between the subjective day and night ($p = 0.0004$; Figure1M,N).

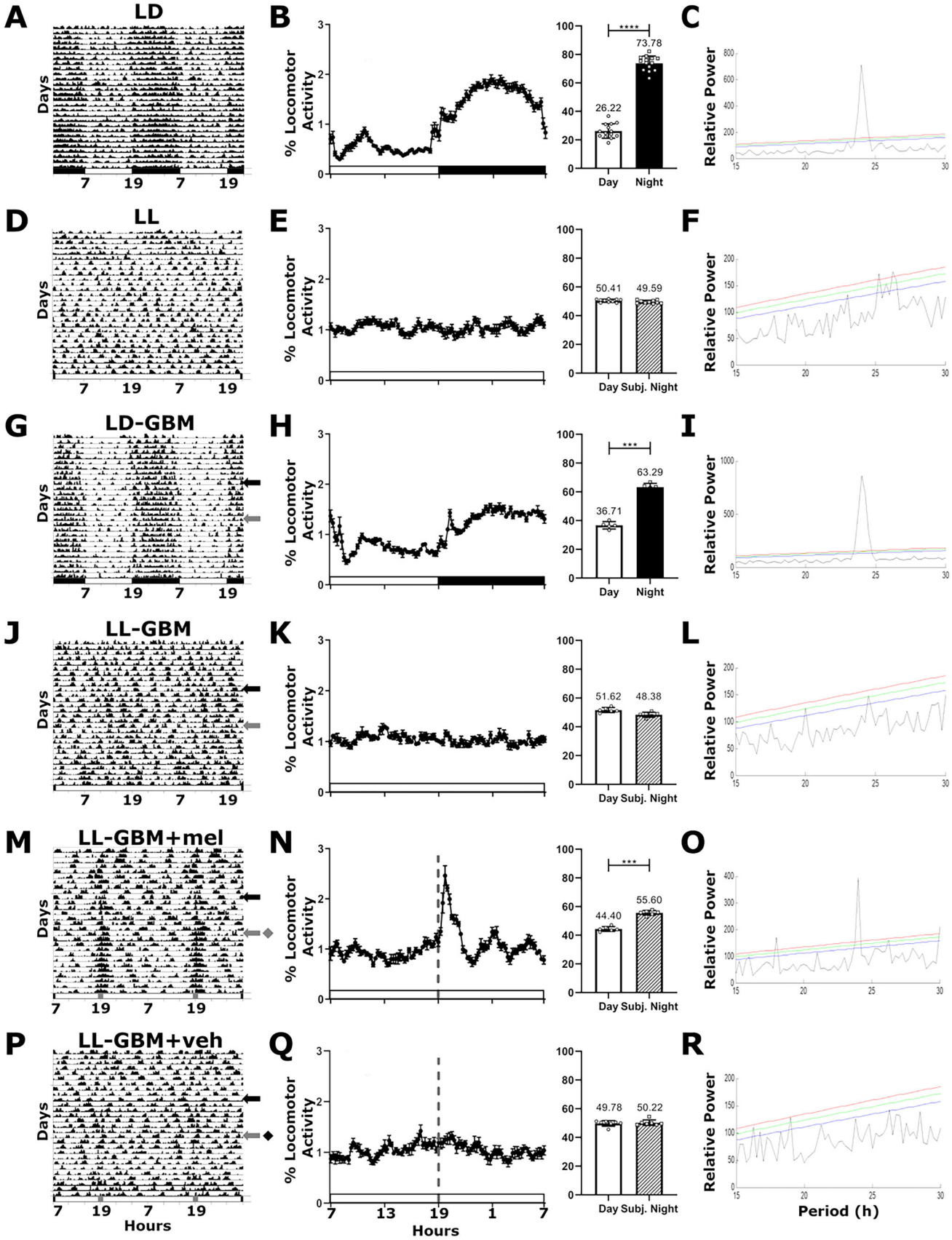

FIGURE 1 | Legend on next page.

This peak was not observed in the LL-GBM-veh group (Figure 1P–R). The periodograms indicated that LD, LD-GBM, and LD-GBM-mel showed 24 h of locomotor activity (Figure 1C,I,O). At the same time, no periodicity was found in LL and LL-GBM, and LL-GBM-veh groups (Figure 1F,L,R). In contrast, although there was no significant difference on average body temperature between the subjective day and night in LL-GBM-mel animals, an overall increase in body temperature was observed following melatonin administration (Figure 2I,J).

3.2 | Melatonin Levels

Melatonin levels were elevated during the night in both LD and LD-GBM groups, reaching their peak at ZT18. In contrast, the LL and LL-GBM groups exhibited a complete loss of melatonin rhythmicity, with consistently low levels throughout the 24-h cycle (Figure 3A). Interestingly, in the LL-GBM-mel group, plasma melatonin levels displayed a significant peak at ZT12 and remained markedly elevated until ZT18 (Figure 3A). The Two-way ANOVA indicated significant effects of photoperiod [$F\ (4100) = 75.45$; $p < 0.001$], time of day [$F\ (4100) = 41.55$; $p < 0.0001$], and their interaction [$F\ (16,100) = 23.05$; $p < 0.0001$].

3.3 | Melatonin Inhibited Tumor Growth in Rats Exposed to Constant Light

Results showed that LL-GBM rats developed significantly larger tumors than LD-GBM starting 13 days after tumor cells inoculation ($p = 0.0001$; Figure 3B). Interestingly, the tumors in LL-GBM-mel rats showed similar growth to those in LD-GBM animals (Figure 3B). The tumor weight of LL-GBM rats was significantly higher than both LD-GBM and LL-GBM-mel groups ($p = 0.0138$; Figure 3C), as observed in the representative picture (Figure 3D).

3.4 | Melatonin Reestablished the Circadian Rhythm of *Per2* in the Liver

In the LD rat's liver, *Per2*, *Bmal1*, *Rorα*, and *Rev-erbα* mRNAs showed a circadian rhythm, with higher levels during the dark middle phase for *Per2* ($p = 0.0001$; Figure 4A), at the beginning of the light phase for *Bmal1* ($p = 0.0003$; Figure 4D), and the light-dark transition for *Rorα* ($p = 0.0004$; Figure 4G) and *Rev-erbα* ($p = 0.0010$; Figure 4J). The mRNA clock genes of LD-GBM rats exhibited a similar circadian pattern as the LD group except for *Rorα*, which lost rhythmicity (Figure 4H). The circadian rhythm of *Per2*, *Bmal1*, and *Rorα* was lost in the LL (Figure 4A,D,G) and the LL-GBM groups (Figure 4B,E,H). In contrast, *Rev-erbα* showed a 6-h phase delay in the subjective night in the LL group ($p = 0.0082$; Figure 4J), and the LL-GBM group displayed a circadian pattern with a peak at the beginning of the subjective day ($p = 0.0099$; Figure 4K). Melatonin administration in the LL-GBM-mel group reestablished the *Per2* circadian rhythm but with an opposite phase compared with LD and LD-GBM ($p = 0.0179$; Figure 4B). In this group, *Bmal1*, *Rorα*, and *Rev-erbα* did not display a rhythm (Figure 4E,H,K).

3.5 | Tumor Tissue Displayed a Unique Pattern of Clock Gene Expression

In the LD-GBM group, *Per2*, *Bmal1*, and *Rorα* mRNA expression in the tumor tissue did not display rhythms (Figure 4C,F,I); only *Rev-erbα* showed a circadian rhythm with a peak at the onset of the dark phase ($p = 0.0241$; Figure 4L). Interestingly, all the clock genes exhibited a circadian rhythm in the tumor tissue of LL-GBM, with the highest point of the curve at the middle of the subjective night for *Per2* ($p = 0.0095$; Figure 4C), at the beginning of the subjective night for *Bmal1* ($p = 0.0224$; Figure 4F), and the subjective day-night transition for *Rorα* ($p = 0.0049$; Figure 4I) and *Rev-erbα* ($p = 0.0162$; Figure 4L). On the other hand, none of the analyzed genes showed rhythmicity in the LL-GBM-mel group (Figure 4C,F,I,L).

3.6 | *p53* in the liver is not affected by the presence of tumors or constant light

In the liver, *p53* expression did not show rhythmicity in any group (Figure 5A,B). The *p21* mRNA was arrhythmic in LD (Figure 5D), but in the LD-GBM group, it exhibited a circadian pattern with a peak at the beginning of the day ($p = 0.0002$; Figure 5E). Whereas in LD ($p = 0.0002$; Figure 5G) and LD-GBM groups ($p = 0.0001$; Figure 5H), *Cyclin E* mRNA showed a circadian rhythm with higher levels at the beginning of the dark phase. In contrast, in the LL group, *p21* expression displayed higher levels at light-dark transition ($p = 0.0245$; Figure 5D) and an antiphase rhythm in *Cyclin E* ($p = 0.0033$; Figure 5G) concerning the LD group. Likewise, in LL rats, the LL-GBM group only displayed rhythmicity in *p21* and *Cyclin E* mRNAs ($p = 0.0001$; Figure 5E,H). In LL-GBM-mel rats, melatonin administration restored a *Cyclin E* circadian pattern like the LD-GBM group, showing a maximal point at the beginning of the subjective night ($p = 0.0043$; Figure 5H). Furthermore, *p21*

FIGURE 1 | Exogenous melatonin partially restores the circadian pattern of locomotor activity in rats exposed to constant light. Representative actograms (left column), daily locomotor activity profiles corresponding day versus night (subjective night) mean comparisons (middle column), and χ^2 periodogram (right column) for each experimental group. Light-Dark (LD; A–C; $n = 14$), Constant light (LL; D–F: $n = 12$); Light-Dark with Glioblastoma (LD-GBM; G–I; $n = 8$); Constant light with Glioblastoma (LL-GBM; J–L; $n = 8$), Constant light with Glioblastoma plus melatonin (LL-GBM-mel; M–O; $n = 10$), and Constant light with Glioblastoma plus vehicle (LL-GBM-veh; P–R; $n = 8$). White and black bars on the *x*-axis represent light (or subjective day) and dark (or subjective night) phases, respectively. Locomotor activity data are presented as mean ± SEM. Gray rhombi and squares in M and P denote the light period; the dotted line in N and Q represents melatonin or vehicle administration timing. Black arrows on the actograms (G, J, M, P) indicate the day of cancer cell injection; gray arrows represent the beginning of tumor measurement. "*" denotes statistically significant differences between night or subjective night versus day, respectively, $p > 0.05$. In periodograms, lower, middle, and upper thresholds correspond to significance levels of $p > 0.1$, 0.05, and 0.01, respectively.

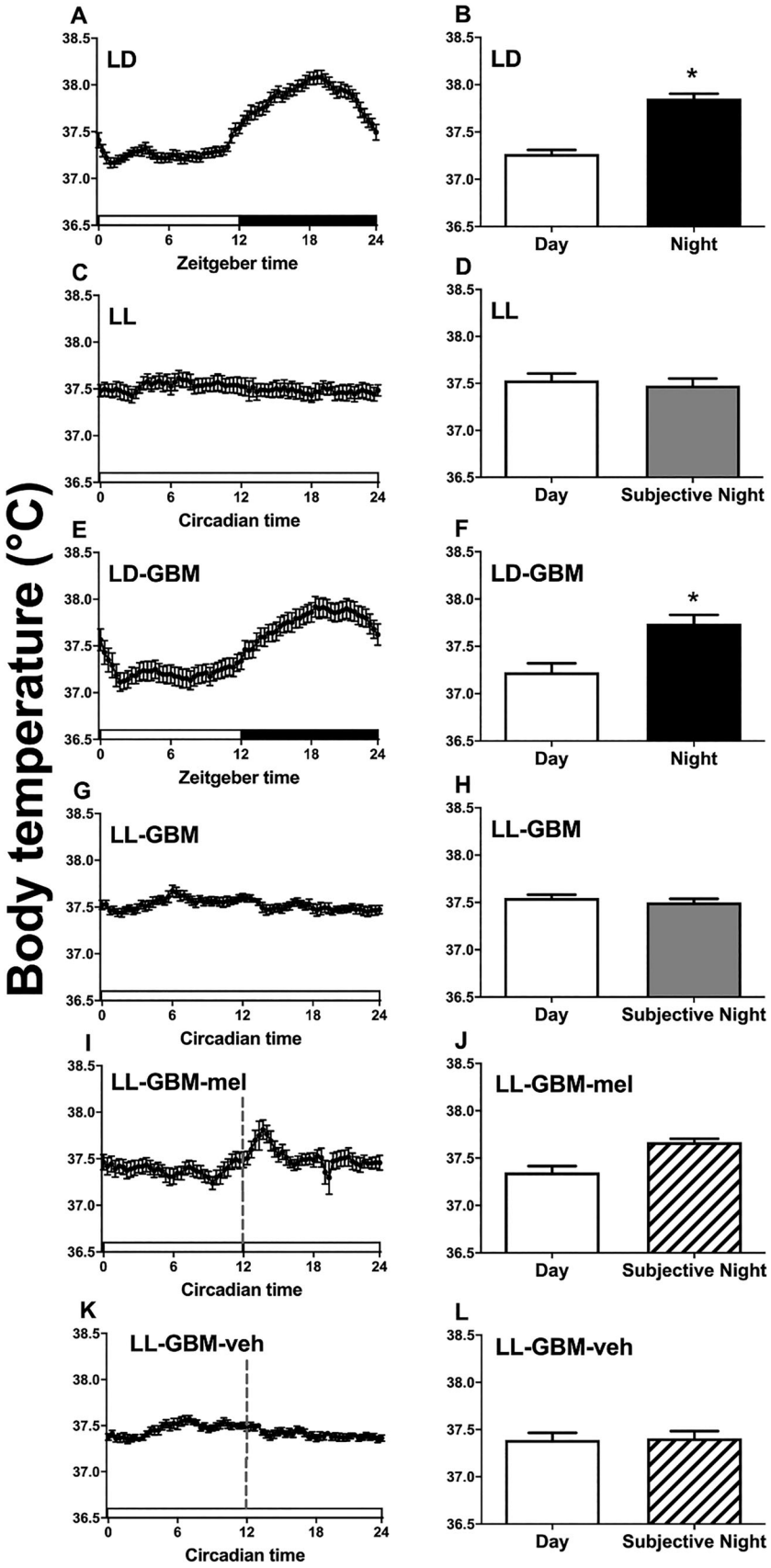

FIGURE 2 | Constant light suppresses the circadian rhythm of body temperature. Daily body temperature profiles (left column) and a day versus night (subjective night) averages (right column) are shown for the following groups: LD(A, B; $n = 15$), LL (C, D; $n = 14$), LD-GBM (E, F; $n = 15$), LL-GBM (G, H; $n = 12$), LL-GBM-mel (I, J; $n = 12$) and LL-GBM-veh (K, L; $n = 8$). White and black bars represent light and dark (or subjective) phases, respectively. Data are presented as mean ± SEM. The gray dotted line in panels I and K represents the timing of melatonin or vehicle administration (CT12). "*" indicates significant differences between night and subjective night versus day, $p > 0.05$.

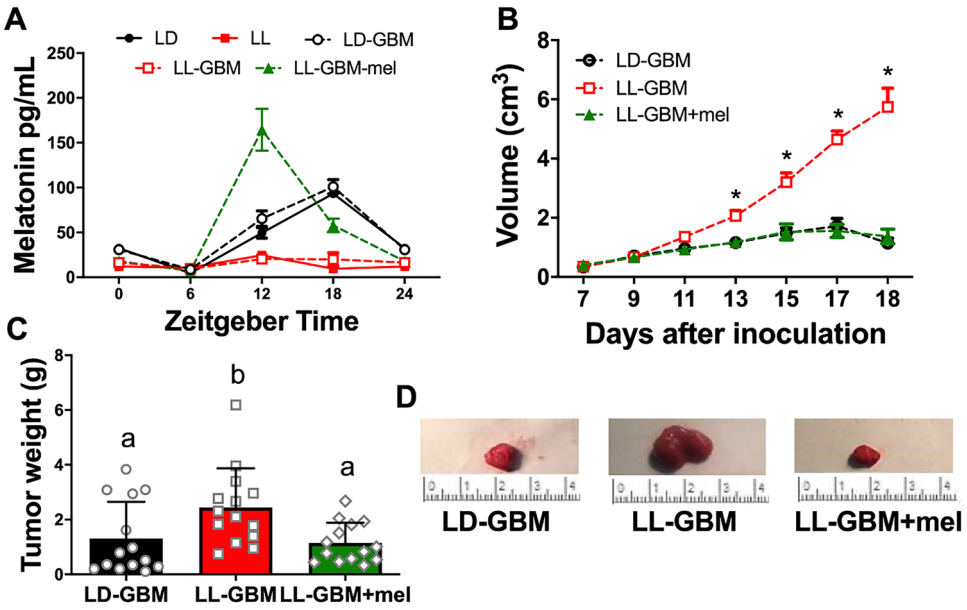

FIGURE 3 | Melatonin administration inhibits tumor growth exacerbated by constant light exposure. (A) Plasma melatonin concentrations throughout the day. (B) Tumor volume growth (cm^3). (C) Final tumor weights in LD-GBM ($n = 17$), LL-GBM ($n = 14$), and LL-GBM-mel ($n = 14$) groups. (D) Representative tumor images from each group at the end of the experimental period. "*" indicates significant differences between LL-GBM versus LD-GBM and LL-GBM- mel, $p > 0.05$. Different letters denote statistically significant group differences ($p > 0.05$).

mRNA maintains high levels during the day, displaying a peak response 6 h after the LD-GBM and LL-GBM groups ($p = 0.0023$; Figure 5E).

3.7 | Melatonin Imposed a Circadian Rhythm of *P53* in Tumor Tissue

In tumor tissue from LD-GBM and LL-GBM groups, cell cycle genes (*p53*, *p21*, and *Cyclin E*) did not display circadian rhythmicity, showing that their expression does not respond to the photoperiod (Figure 5C,F,I). On the other hand, melatonin induced a circadian pattern in *p53*, reaching its highest levels at the beginning of the subjective night ($p = 0.0043$; Figure 5C), but not for *p21* and *Cyclin E* mRNAs (Figure 5F,I).

3.8 | Constant Light Does Not Affect the Rhythmicity of *VEGF-A*, *PDFG-C*, and *Tnf-α* in the Liver

The hepatic expression of *VEGF-A*, *PDGF-C*, *TNF-α*, and *Ang* showed a circadian rhythm in LD animals. The highest point of the curve of *VEGF-A* ($p = 0.0016$; Figure 6A) and *Ang* ($p = 0.0014$; Figure 6J) was observed at ZT0, while *PDGF*-C ($p = 0.0015$; Figure 6D) and *TNF-α* ($p = 0.0001$; Figure 6G) were at ZT6 and ZT18, respectively. Also, in the LD-GBM group, the expression of all the proangiogenic genes exhibited a circadian pattern, *VEGF-A* ($p = 0.0001$; Figure 6B) and *TNF-α* ($p = 0.0098$; Figure 6H) peaked at ZT18 and ZT6, while the peaks of *PDGF-C* ($p = 0.0496$; Figure 6E) and *Ang* ($p = 0.0095$; Figure 6K) reached the maximal expression at ZT12 and ZT0, respectively. LL animals displayed inverted rhythm for *VEGF-A* ($p = 0.0199$) and *TNF-α* ($p = 0.0162$; Figure 6A,G), a 6-h phase advance in *PDGF-C* ($p = 0.0126$; Figure 6D), and arrhythmicity in *Ang* expression (Figure 6J) compared to the LD group. Likewise, in the LL-GBM group, *VEGF-A* ($p = 0.0025$) and *TNF-α* ($p = 0.0014$) presented a circadian pattern; nevertheless, *both* inverted the rhythm in the LD-GBM group (Figure 6B,H). On the other hand, *PDGF*-C and *Ang* did not show circadian rhythm (Figure 6E,K). In LL-GBM-mel, melatonin administration reestablished rhythmic patterns for all proangiogenic genes. *VEGF-A* is in phase with LD-GBM (Figure 6B), *PDGF-C* and *Ang* displayed a 6-h delay ($p = 0.0198$ and $p = 0.0100$; Figure 6E,K), while *TNF-α* presented a 12-h delay ($p = 0.0154$; Figure 6H).

3.9 | Proangiogenic Genes Did Not Show a Circadian Rhythm in Tumor Tissue of the LD-GBM Group, Except *PDFG-C*

In the LD-GBM group, the mRNA of *VEGF-A*, *TNF-α*, and *Ang* in the tumor tissue did not display a circadian pattern (Figure 6C,I,L); only *PDGF-C* exhibited a maximum expression at ZT12 ($p = 0.046$; Figure 6F). Interestingly, *Ang* ($p = 0.0327$; Figure 6L) and *PDGF-C* ($p = 0.0009$; Figure 6F) presented a circadian rhythm in the tumors of LL-GBM rats despite constant light, but *VEGF-A* and *TNF-α* maintained arrhythmic (Figure 6C,I). Melatonin entrained *TNF-α* expression, which peaked 6 h before hormone administration ($p = 0.0154$; Figure 6I), while *VEGF-A*, *PDGF-C*, and *Ang* expression were arrhythmic (Figure 6C,F,L).

3.10 | Melatonin Inhibits Angiogenesis in the Ll Conditions

To explore angiogenesis as a marker of tumor progression, the changes in the number and luminal area of blood vessels in the tumoral tissue from LD-GBM, LL-GBM, and LL-GBM-mel animals were compared. The number of blood vessels in the tumor

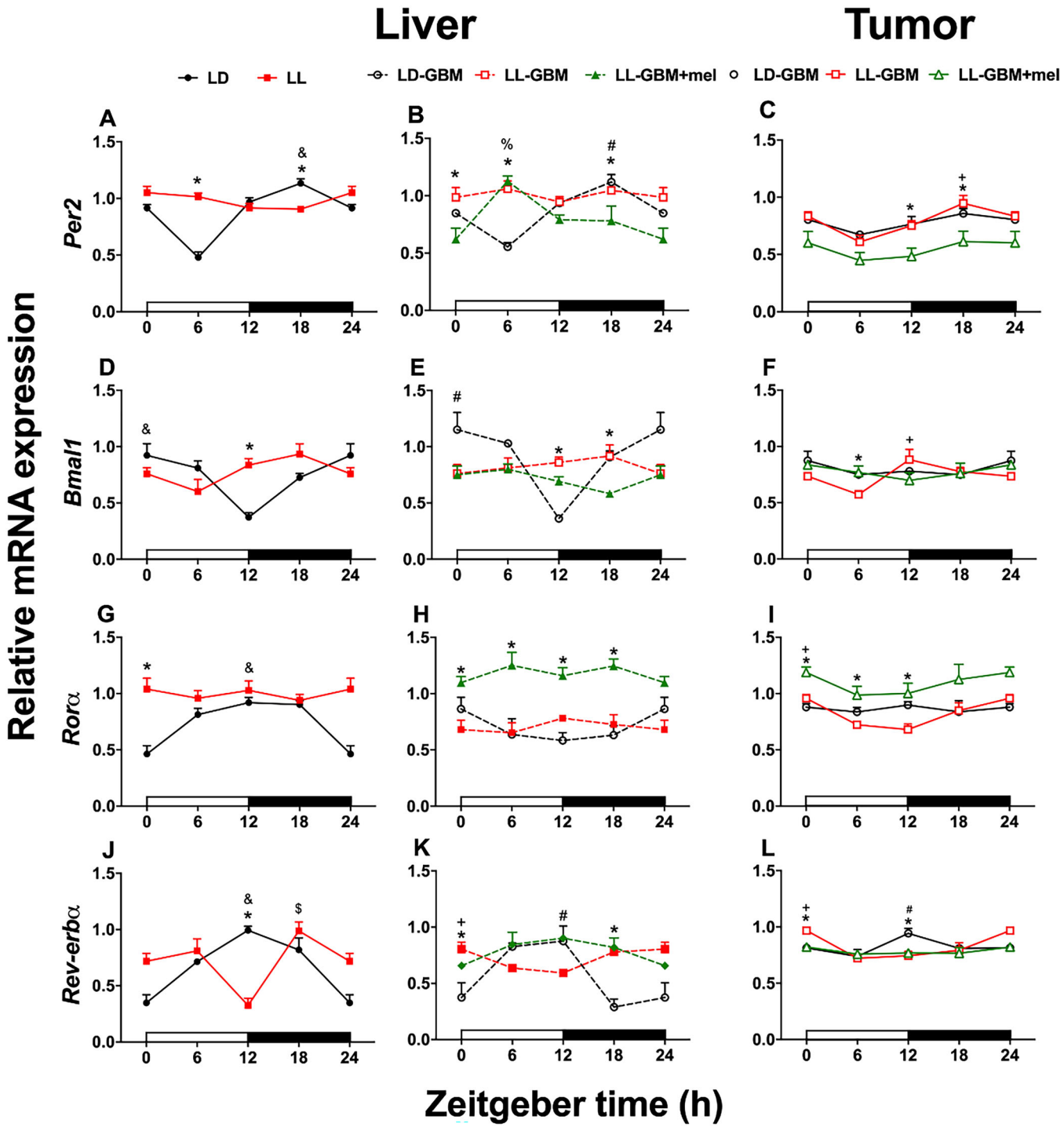

FIGURE 4 | Constant light and glioblastoma modify the circadian rhythm pattern of hepatic and tumoral clock genes. Temporal profiles of clock gene mRNA expression (*Per2*, *Bmal1*, *Rorα*, and *Rev-erbα*) in the liver of nontumor groups (LD, LL; A, D, G, J), glioblastoma-bearing groups (LD-GBM, LL-GBM, LL-GBM-mel;B, E, H, K), and tumor tissue (tumor-bearing only; C, F, I, L). Gene expression normalized to Gapdh. Sample size: $n = 3$–4 rats per time point. White bars: Light period; Black bars: Dark period. Circadian rhythms are represented as: & (LD), $ (LL), # (LD-GBM), + (LL-GBM), % (LL-GBM-mel); $p > 0.05$. "*" indicates significant differences between groups at the same time point (see Supporting Information S6: Table 1). Melatonin administration was in ZT12.

tissue was significantly higher in LD-GBM than in LL-GBM and LL-GBM-mel ($p < 0.001$; Figure 7A,C). In addition, melatonin promoted a significant increase in LL-GBM-mel vascularization regarding the LL-GBM group ($p < 0.05$; Figure 7A,C). Nevertheless, a blood vessel in the LD-GBM group (621.4+/−60.8 μm^2) was significantly smaller than in the LL-GBM group (12484.5+/−2369 μm^2, $p < 0.001$; Figure 7B,C). Interestingly, in the LL-GBM-mel, melatonin administration reduced the size of the blood vessels to similar values as the LD-GBM group (1959.1+/−352 μm^2; Figure 7B).

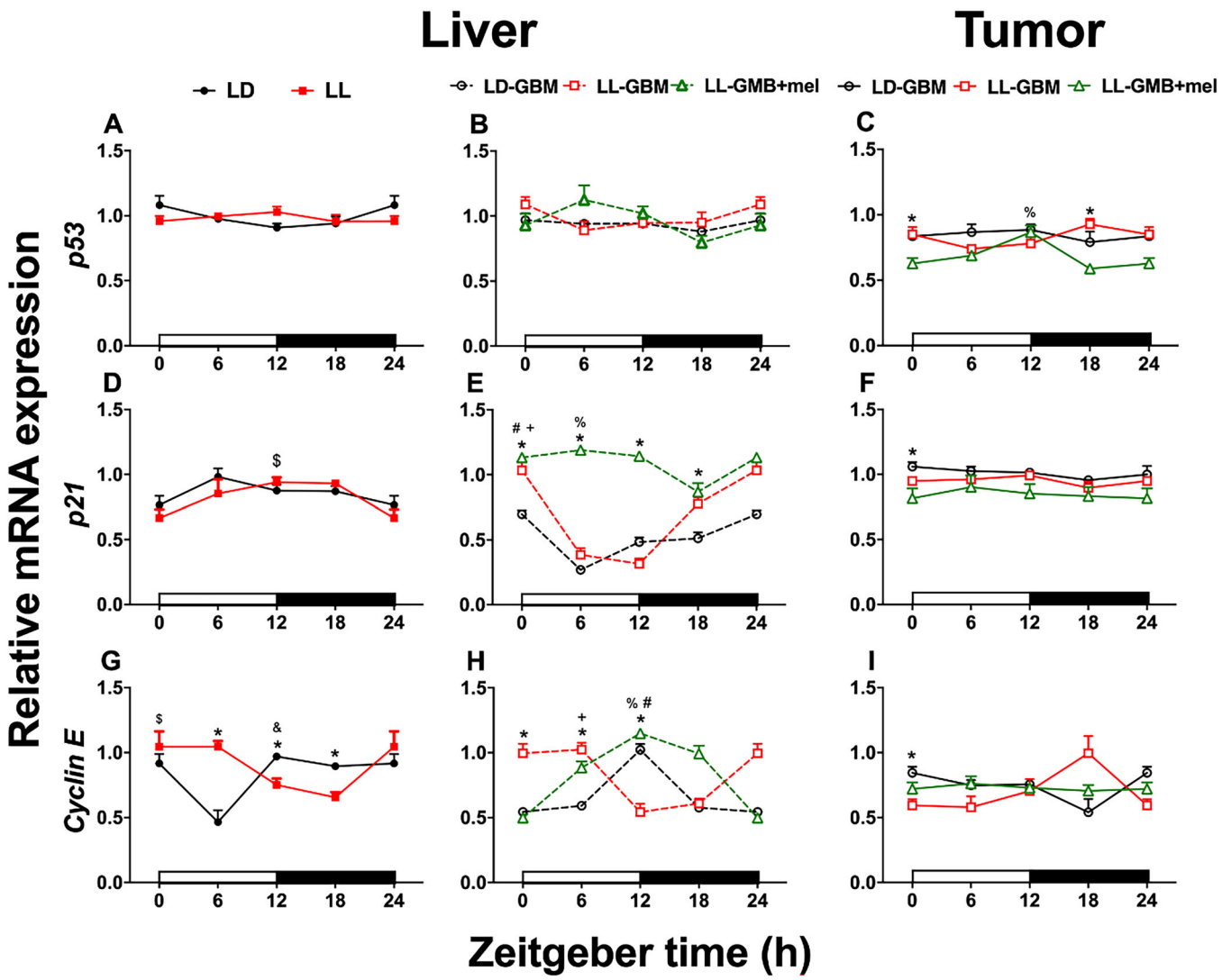

FIGURE 5 | Melatonin administration imposes circadian rhythmicity in cell cycle gene expression in liver and tumor tissues. Relative expression of *p21* and *Cyclin E* in the liver (A, B, D, E, G, H) and *p53* in tumor tissue (C, F, I) across 24 h in LD, LL, LD-GBM, LL-GBM, and LL-GBM-mel groups. Each value represents mean ± SEM ($n = 3$–4 per time point). "*" indicates statistically significant differences between groups at the same point. Other figure elements are in Figure 4.

3.11 | Melatonin Administration Failed to Entrain *Mt1r* and *Mt2r* Expression in the Liver and Tumor Tissue

In the liver of the LD group, *Mt1r* and *Mt2r* mRNAs showed a circadian rhythm, with peak levels observed at ZT0 ($p = 0.0009$ and 0.0079; Figure 8A,D). In LD-GBM, *Mt1r* presented the same peak as LD (ZT0, $p = 0.0001$; Figure 8B), while *Mt2r* was in antiphase (ZT12; $p = 0.0076$; Figure 8E). In both groups of animals exposed to constant light (LL and LL-GBM), *Mt1r* exhibited daily oscillation; in LL presented 6 h phase delay ($p = 0.0173$; Figure 8A), while in LL-GBM the highest point of the curve did not change concerning the LD-GBM ($p = 0.0042$; Figure 8B). In contrast, *Mt2r* gene lost the circadian rhythm in both groups (Figure 8D,E). In the LL-GBM-mel group, melatonin receptors did not present rhythmicity (Figure 8B,E). The tumor tissue of the LL-GBM group presented a circadian rhythm in the mRNA expression of *Mt1r* ($p = 0.0032$; Figure 8C) and *Mt2r* ($p = 0.0055$; Figure 8F). On the contrary, both genes in the LD-GBM and LL-GBM-mel groups were arrhythmic (Figure 8C,F).

4 | Discussion

Although several studies have demonstrated that melatonin offers protective effects against various diseases, including multiple types of cancer, diabetes, obesity, and gastrointestinal and immune disorders, the size of the effect and the mechanism remain subject to ongoing debate. In the current study, we demonstrated that melatonin prevents malignant progression in primary cultures of glioblastoma-like stem cells, suggesting that melatonin inhibits tumor cell proliferation. Furthermore, melatonin´s effects on circadian rhythm regulation, cell cycle progression, and angiogenesis have been explored independently. Our data provide evidence that melatonin restricts glioblastoma progression by decreasing the vascularized area within the tumor, possibly through upregulation of *Mt1r* and *Rorα*, suggesting new molecular pathways involved in tumor growth regulation. Interestingly, we also observed that the glioblastoma cells impose a circadian rhythm in some cell cycle and angiogenic genes under constant light. These findings could have significant implications for cancer treatment and prevention,

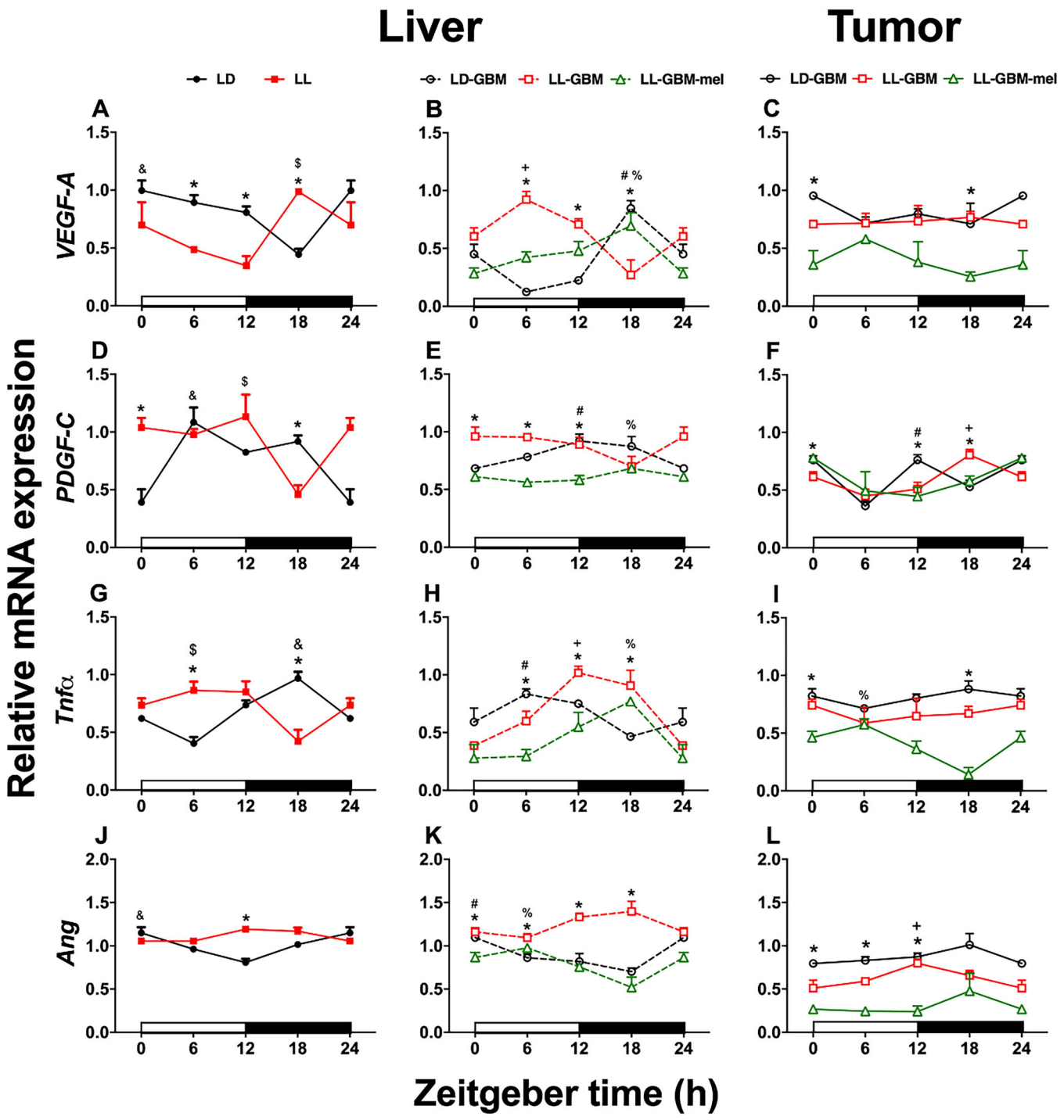

FIGURE 6 | Melatonin induces circadian rhythmicity in hepatic but not tumoral expression of proangiogenic genes. Temporal expression profiles of *VEGF*-A, *PDGF-C*, *TNF-α*, and *Ang* in the liver (A, B, D, E, G, H, J, K) and tumor (C, F, I, L) of LD, LL, LD-GBM, LL-GBM, and LL-GBM-mel groups. Data are presented as mean ± SEM (n = 3–4 per time point). "*" indicates statistically significant differences between groups at the same point. For additional features, see Figure 4.

providing a new avenue for research and potential therapeutic strategies.

To validate the circadian disruption induced by constant light and evaluate melatonin entraining effect, we recorded the locomotor activity and core body temperature in desynchronized animals. As previously reported, groups under the LD cycle displayed high body temperature during the dark phase compared to the light phase. In contrast, animals under constant light showed arrhythmicity in locomotor activity and body temperature patterns [16, 17]. However, the animals under the LL-GBM-mel protocol presented a peak of locomotor activity synchronized with the time of melatonin administration, as previously reported [18, 19]. This result indicates that the locomotor activity rhythmicity was improved by melatonin treatment. Similarly, body temperature in LL-GBM-mel animals showed a peak following melatonin administration; however, melatonin did not induce a circadian rhythm, likely because

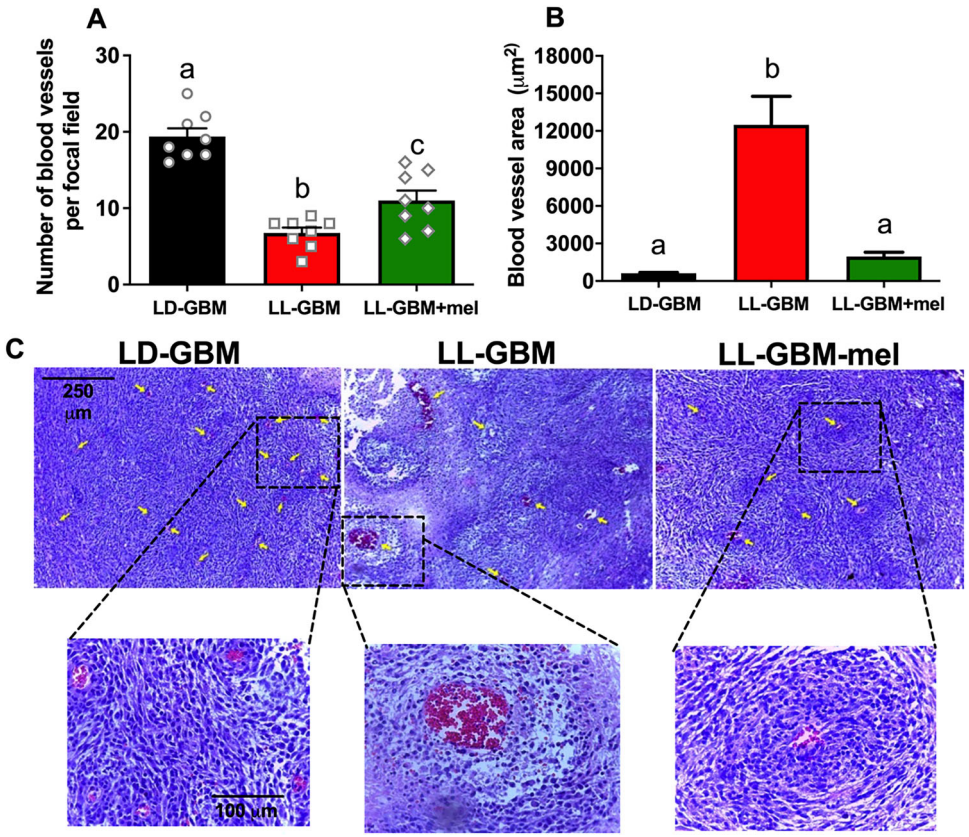

FIGURE 7 | Melatonin attenuates angiogenesis in tumors by reducing the number and area of blood vessels under constant light exposure. Quantification of (A) number ($n = 8$) and (B) area ($n = 15$) of blood vessels in tumor tissue from LD-GBM, LL-GBM, and LL-GBM-mel groups. (C) Representative hematoxylin-eosin-stained section of tumor tissue at 10× and 40× magnifications. Data are presented as mean ± SEM. Different letters indicate statistically significant differences ($p > 0.05$).

ultradian rhythms predominate under constant light conditions [20].

Several studies have demonstrated that tumor growth is promoted by disruption of the circadian rhythm [21–23] and reduced nocturnal melatonin production [24–26]. In this context, we demonstrated that arrhythmicity induced by constant light increases tumor growth, which is consistent with previous reports [09-10,16,21-23]. Furthermore, we confirmed that melatonin administration inhibits cancer cell proliferation in rats exposed to continuous light, likely due to its protective role against several types of cancer and its synchronizing effects [27].

To investigate whether the protective and antitumoral effects of melatonin under constant light conditions are linked to alterations in the molecular clock, we analyze the circadian expression of clock genes. Consistent with previous reports, hepatic expression of clock genes exhibited a circadian rhythm under LD photoperiod [28–30]. However, *Rorα* lost rhythmicity in the LD-GBM group, suggesting that chemokines, cytokines, and growth factors secreted by glioma cells may disturb its expression [31]. As expected, constant light exposure abolished the circadian expression of *Per2*, *Bmal1*, and *Rorα*. In contrast, *Rev-erbα* maintained rhythmicity, potentially due to glucocorticoid secretion, which can transcriptionally downregulate *Rev-erbα* expression [32–34]. In our study, melatonin administration did not restore circadian rhythms of *Bmal1*, *Rorα*, and *Rev-erbα* expression in either liver or tumor tissue under constant light or cancer conditions. A remarkable exception was the expression of *Per2* in the liver, which displayed a circadian pattern in the LL-GBM-mel group, with mRNA levels restored to those comparable to the LD photoperiod (Supporting Information S2: Figure 2A). However, this effect was absent in tumor tissue (Supporting Information S2: Figure 2E). Interestingly, melatonin increased *Rorα* expression levels in both liver and tumor tissues compared to all other groups (Supporting Information S2: Figure 2C,G). This finding is significant given the role of *Rorα* as a tumor suppressor and prognostic marker in hepatocellular carcinoma [35], suggesting that *Rorα* may contribute to reduced tumor mass in glioblastoma through melatonin. Moreover, melatonin might exert its protective biological effects via nuclear signaling pathways involving RZR/ROR nuclear receptors in peripheral tissues [36, 37]. Overall, these results confirm that constant light disrupts clock gene synchronization. At the same time, melatonin can modulate the rhythm and expression levels of these genes in the liver and, to a lesser extent, in glioblastoma.

Cell cycle progression is a key biological process regulated by circadian rhythms, and it is particularly relevant in the context of cancer. Several reports have demonstrated that *p21* expression is regulated by core clock components such as *Bmal1*, *Rorα*, *Rev-erbα*, as well as melatonin [28–30]. Additionally, *p53* promotes *p21* expression while reducing Cyclin E levels, and together, these proteins play critical roles in cell cycle

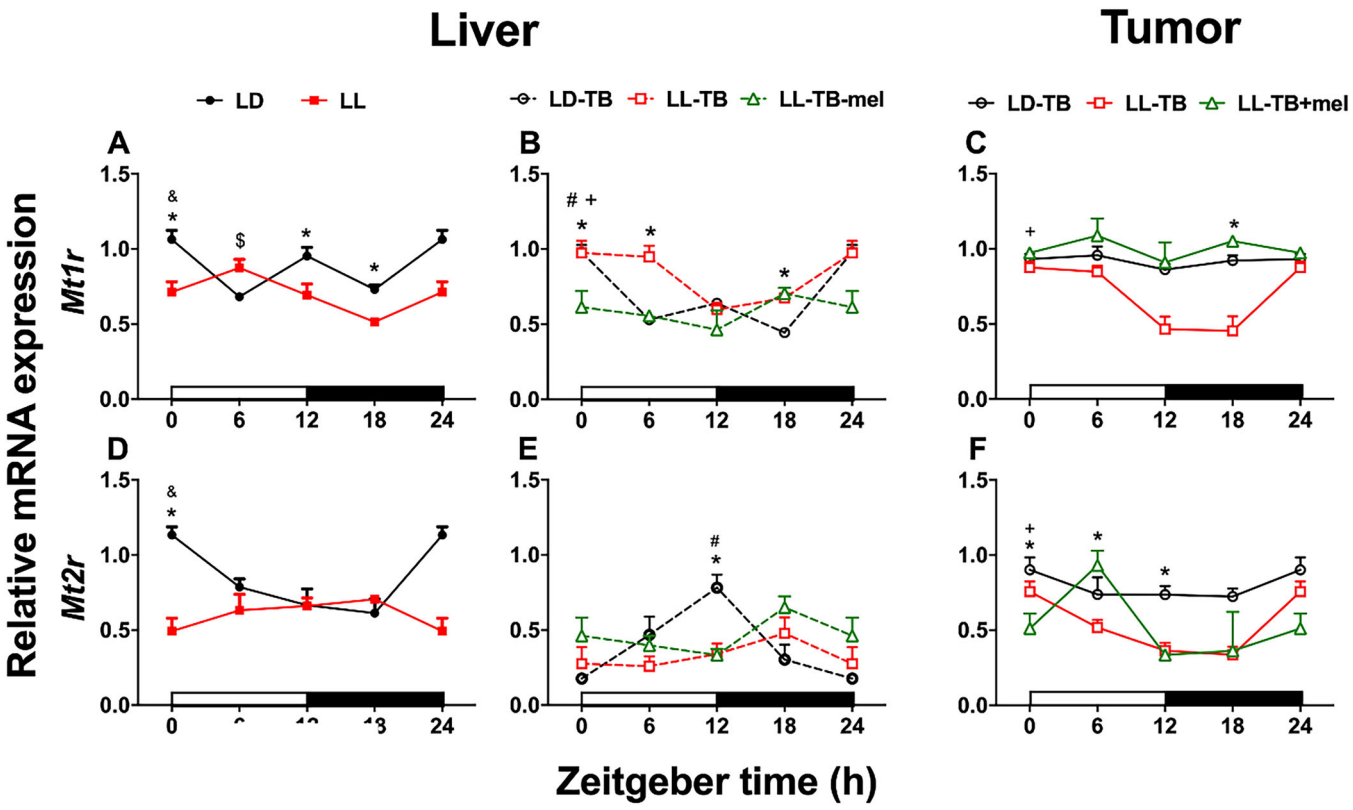

FIGURE 8 | Constant light exposure induces circadian expression of melatonin receptors in tumor tissue. Relative daily expression of *Mt1r* and *Mt2r* in liver (A,B,D,E) and tumor (C, F) tissues from LD, LL, LD-GBM, LL-GBM, and LL-GBM-mel groups. Each value represents mean ± SEM ($n = 3$–4 per time point). "*" indicates statistically significant differences between groups at the same time point. For additional figure features, see Figure 4.

regulation [29, 30, 38]. Furthermore, *Per2* and *p53* reciprocally modulate their expression [30]. In our study, we did not observe circadian rhythmicity or significant changes in *p53* expression in the liver across any experimental group (Supporting Information S3: Figure 3A), despite the presence of *Per2* rhythmicity and altered expression levels over 24-h. This lack of p53 modulation may be due to multiple cellular stresses that induce its transcription independently of circadian control [39].

Interestingly, although constant light and tumor presence disrupted several clock-controlled processes, *p21* and *Cyclin E* show a rhythm in the liver but not in tumor tissue. Melatonin administration further enhanced the rhythmic expression of *p21* and increased its overall levels in the liver (Supporting Information S3: Figure 3B). This effect may be related to the observed increase in *Rorα* expression, supporting the hypothesis that *p21* regulation can occur through a p53-independent pathway mediated by circadian clock components [39, 40]. These findings support the idea that melatonin exerts a protective effect in peripheral tissues by modulating cell cycle regulators via circadian mechanisms. However, this protective role was not observed in tumor tissue (Supporting Information S3: Figure 3F). Previous studies have reported that melatonin can downregulate *p21* expression in rat glioma cells, highlighting potential tissue-specific responses to melatonin and the complexity of its antitumor actions [40].

The angiogenic phenotype of gliomas is closely associated with tumor malignancy, patient survival, and clinical recurrence [41]. In the current study, we observed that *VEGF-A*, *PDGF*-C, *TNF-α*, and *Ang* exhibited circadian rhythmicity under LD photoperiod conditions. These genes maintained similar levels across 24 h in the liver, except VEGF-A (Supporting Information S4: Figure 4A–D) [16, 42, 43]. Surprisingly, *VEGF-A* and *TNF-α* maintained their circadian rhythm under constant light, while *PDGF-C* exhibited rhythmic expression only in the LL group. In contrast, *Ang* lost its rhythmicity in both conditions. These findings suggest that specific proangiogenic genes respond to internal signals capable of maintaining circadian regulation even under chronodisruptive conditions such as constant light exposure. Previous studies have supported the role of melatonin in modulating angiogenesis in both physiological and pathological contexts [27, 44, 45]. Consistent with this, we observed that melatonin administration (LL-GBM-mel) reestablished circadian rhythms for all proangiogenic genes and significantly decreased the expression of *VEGF-A* and *PDGF-C* in hepatic and tumor tissues, respectively (Supporting Information S4: Figures 4A and 3B). We observed a similar downregulation effect in tumor tissue, although *PDGF-C* expression remained unaffected (Supporting Information S4: Figure 4E–H). These results suggest that melatonin may exert its antiangiogenic functions by modulating the expression and rhythmicity of key proangiogenic genes in both peripheral and tumor environments. This supports the idea that melatonin contributes to tumor suppression through circadian resynchronization and direct regulation of angiogenesis-related pathways.

We also observed that constant light exposure decreases the number of blood vessels compared to the LD group. Interestingly, the vessel area in LL-GBM animals was greater than in LD-GBM and LL-GBM-mel groups. This result suggests two possible interpretations: first, that constant light may promote tumor growth by increasing vascularization, thereby providing more nutrients to the tumor; and second, that melatonin may exert its antitumor effects by inhibiting the expansion of the vascular area, likely through the downregulating of proangiogenic factors, as we previously demonstrated. Melatonin has been reported to inhibit the development of various cancer types [46] and to suppress microvessel formation within tumors [44, 47, 48]. These effects have been proposed to occur through the inhibition of multiple proangiogenic components, supporting the idea that the antitumor effect of melatonin is closely linked to its regulation of angiogenesis [44, 45, 49].

Finally, we assessed the mRNA expression of *Mt1r* and *Mt2r*, which exhibited circadian rhythmicity in the liver under LD photoperiod. Although the peak expression differed slightly from that reported by Venegas et al. (2012), variations are expected, given that receptor expression can be influenced by factors such as tissue type, species, and time of day, among others [50]. As expected, constant light exposure (LL and LL-GBM groups) disrupted the circadian rhythm of *Mt2r* in hepatic tissue, whereas *Mt1r* maintained rhythmic expression regardless of continuous light or tumor presence. Unlike previous reports, melatonin administration in this setting was insufficient to reestablish a circadian rhythm or restore the expression levels of both genes over 24 h (Supporting Information S5: Figure 5A,B). It is worth noting that both constant light and pinealectomy have been shown to reduce Mt1r/Mt2r expression levels in a similar manner [50].

Moreover, we observed that Mt1r and Mt2r expression in glioblastoma did not display a circadian rhythm in either the LD-GBM and LL-GBM-mel groups, despite the presence of both endogenous and exogenous melatonin. Interestingly, the melatonin administration selectively restored the expression of *Mt1r* but not *Mt2r* (Supporting Information S5: Figure 5C,D). Previous studies have shown that overexpression of the MT1 receptor is associated with enhanced melatonin-mediated growth suppression in various cancer types [51], potentially through the inhibition of cAMP production [52]. In contrast, Martin et al. reported that melatonin suppresses glioma cell proliferation by inhibiting the activation of PKC and NF-κB [52]. These controversial results underscore the complexity of the melatonin mechanisms of action and suggest the involvement of multiple signaling pathways. Our data support the idea that one potential mechanism by which melatonin inhibits tumor growth is through upregulation of MT1R, which may, in turn, reduce linoleic acid uptake by cancer cells [51]. A major limitation of our study is the lack of data on the effects of melatonin administration in GBM under untreated LD and LL conditions. Including such comparisons in future studies would provide more comprehensive insights into the role of melatonin in glioblastoma progression.

In summary, this study provides evidence that melatonin reduces the glioblastoma tumor growth, by decreasing the tumor's blood vessel area, which is potentially linked to increased expression of transmembrane receptors such as *Mt1r*. These require to be investigated deeply in further studies. Our findings contribute to the understanding of how melatonin modulates gene expression involved in the molecular pathways that connect cancer initiation and progression, angiogenesis, and circadian disruption. These insights may support the development of novel therapeutic strategies or adjunct treatments aimed at reducing the malignancy of glioblastoma.

Author Contributions

Roberto C. Salgado-Delgado and Nadia Saderi directed the study. Skarleth Cardenas-Romero, Oscar Daniel Ramirez-Plascencia, Adrián Baez-Ruiz, and Omar Flores-Sandoval are responsible for the development of methodology, acquisition, and data analysis. Carolina Escobar Briones provided animals and the C6 glioblastoma cell line. Skarleth Cardenas-Romero, Carolina Escobar Briones, Roberto C. Salgado-Delgado, and Nadia Saderi are responsible for the interpretation of data, writing, and manuscript review. All authors contributed to the discussion of the data and editing of the manuscript.

Acknowledgments

This study was supported by Consejo Nacional de Ciencia y Tecnología, México (CONACyT grant 183078 for RSD; 243298 for NS), FAI 2019 for RSD, FAI 2020 for NS, CONACyT provided a PhD scholarship to SCR (grant 556514). We thank Dr. Jorge Arreola and Q.F.B. Carmen Yudith Hernandez Carballo for their help throughout this study. Open access funding provided by UNAM.

Conflicts of Interest

The authors declare no conflicts of interest.

Data Availability Statement

All data created during this study is openly available in the data repository of the Universidad Autónoma de San Luis Potosí at https://bvu.uaslp.mx, ninive. uaslp. mx/jspui/handle/i/2856.

References

1. A. Sancar and R. N. Van Gelder, "Clocks, Cancer, and Chronochemotherapy," *Science* 371, no. 6524 (2021): eabb0738, https://doi.org/10.1126/science.abb0738.

2. R. J. Reiter, D. X. Tan, A. Korkmaz, et al., "Light at Night, Chronodisruption, Melatonin Suppression, and Cancer Risk: A Review," *Critical Reviews™ in Oncogenesis* 13, no. 4 (2007): 303–328.

3. B. Claustrat and J. Leston, "Melatonin: Physiological Effects in Humans," *Neuro-Chirurgie* 61, no. 2–3 (2015): 77–84, https://doi.org/10.1016/j.neuchi.2015.03.002.

4. F. G. Amaral and J. Cipolla-Neto, "A Brief Review About Melatonin, a Pineal Hormone," *Archives of Endocrinology and Metabolism* 62, no. 4 (2018): 472–479, https://doi.org/10.20945/2359-3997000000066.

5. D. P. Cardinali, P. Delagrange, M. L. Dubocovich, et al., "Melatonin Receptors in Gtopdb V.2023.1," *IUPHAR/BPS Guide to Pharmacology CITE* 2023, no. 1 (2023), https://doi.org/10.2218/gtopdb/F39/2023.1.

6. X. Chen, A. Hao, X. Li, et al., "Melatonin Inhibits Tumorigenicity of Glioblastoma Stem-Like Cells via the AKT–EZH2–STAT3 Signaling Axis," *Journal of Pineal Research* 61 (2016): 208–217, https://doi.org/10.1111/jpi.12341.

7. B. V. Jardim-Perassi, A. S. Arbab, L. C. Ferreira, et al., "Effect of Melatonin on Tumor Growth and Angiogenesis in Xenograft Model of Breast Cancer," *PLoS One* 9, no. 1 (2014): e85311, https://doi.org/10.1371/journal.pone.0085311.

8. J. Menéndez-Menéndez and C. Martínez-Campa, "Melatonin: An Anti-Tumor Agent in Hormone-Dependent Cancers," *International*

Journal of Endocrinology 2018 (2018): 1–20, https://doi.org/10.1155/2018/3271948.

9. V. N. Anisimov, D. A. Baturin, I. G. Popovich, et al., "Effect of Exposure to Light-at-Night on Life Span and Spontaneous Carcinogenesis in Female CBA Mice," *International Journal of Cancer* 111, no. 4 (2004): 475–479, https://doi.org/10.1002/ijc.20298.

10. S. Cos, D. Mediavilla, C. Martínez-Campa, A. González, C. Alonso-González, and E. J. Sánchez-Barceló, "Exposure to Light-at-Night Increases the Growth of DMBA-Induced Mammary Adenocarcinomas in Rats," *Cancer Letters* 235, no. 2 (2006): 266–271, https://doi.org/10.1016/j.canlet.2005.04.025.

11. World Health Organization. Cancer Key Facts, 2020. https://www.who.int/news-room/fact-sheets/detail/cancer.

12. R. Salgado-Delgado, M. Angeles-Castellanos, N. Saderi, R. M. Buijs, and C. Escobar, "Food Intake During the Normal Activity Phase Prevents Obesity and Circadian Desynchrony in a Rat Model of Night Work," *Journal of Clinical Endocrinology & Metabolism* 95, no. 2 (2010): 978–979, https://doi.org/10.1210/jcem.95.2.9987.

13. K. P. Weinfurt, "Repeated Measures Analyses: ANOVA, MONOVA and HLM." in *Reading and Understanding More Multivariate Statistics. Am Psychol Assoc*, eds. L. G. Grimm and P. R. Yarnold (American Psychological Association, 2000), 317–361. https://psycnet.apa.org/record/2000-00427-010.

14. H. Akaike, "A New Look at the Statistical Model Identification," *IEEE Transactions on Automatic Control* 19, no. 6 (1974): 716–723, https://doi.org/10.1109/tac.1974.1100705.

15. R. M. Heiberger and B. Holland, "Multiple Regression—More Than One Predictor," In *Statistical Analysis and Data Display. Springer Texts In Statistics*. Springer. (2015), 263–314,https://doi.org/10.1007/978-1-4939-2122-5_9.

16. N. N. Guerrero-Vargas, R. Navarro-Espíndola, M. A. Guzmán-Ruíz, et al., "Circadian Disruption Promotes Tumor Growth by Anabolic Host Metabolism, Experimental Evidence in a Rat Model," *BMC Cancer* 17, no. 1 (2017): 625, https://doi.org/10.1186/s12885-017-3636-3.

17. M. Ikeda, M. Sagara, and S. Inoué, "Continuous Exposure to Dim Illumination Uncouples Temporal Patterns of Sleep, Body Temperature, Locomotion and Drinking Behavior in the Rat," *Neuroscience Letters* 279, no. 3 (2000): 185–189, https://doi.org/10.1016/s0304-3940(99)00943-x.

18. S. Heigl and E. Gwinner, "Synchronization of Circadian Rhythms of House Sparrows by Oral Melatonin: Effects of Changing Period," *Journal of Biological Rhythms* 10, no. 3 (1995): 225–233, https://doi.org/10.1177/074873049501000305.

19. M. J. Chesworth, V. M. Cassone, and S. M. Armstrong, "Effects of Daily Melatonin Injections on Activity Rhythms of Rats in Constant Light," *American Journal of Physiology-Regulatory, Integrative and Comparative Physiology* 253, no. 1 (1987): R101–R107. https://doi.org/10.1152/ajpregu.1987.253.1.

20. M. E. Diatroptov, M. A. Diatroptova, A. M. Kosyreva, et al., "Ultradian Rhythms of Body Temperatures in Male Wistar Rats Maintained under Conditions of Constant Illumination," *Bulletin of Experimental Biology and Medicine* 167, no. 6 (2019): 735–739, https://doi.org/10.1007/s10517-019-04611-z.

21. E. Filipski, P. Subramanian, J. Carrière, C. Guettier, H. Barbason, and F. Lévi, "Circadian Disruption Accelerates Liver Carcinogenesis in Mice," *Mutation Research/Genetic Toxicology and Environmental Mutagenesis* 680, no. 1–2 (2009): 95–105, https://doi.org/10.1016/j.mrgentox.2009.10.002.

22. I. A. Vinogradova, V. N. Anisimov, A. V. Bukalev, A. V. Semenchenko, and M. A. Zabezhinski, "Circadian Disruption Induced by Light-at-Night Accelerates Aging and Promotes Tumorigenesis in Rats," *Aging* 1, no. 10 (2009): 855–865, https://doi.org/10.18632/aging.100092.

23. T. Papagiannakopoulos, M. R. Bauer, S. M. Davidson, et al., "Circadian Rhythm Disruption Promotes Lung Tumorigenesis," *Cell Metabolism* 24, no. 2 (2016): 324–331, https://doi.org/10.1016/j.cmet.2016.07.001.

24. R. J. Reiter, D. X. Tan, A. Korkmaz, et al., "Light At Night, Chronodisruption, Melatonin Suppression, and Cancer Risk: A Review," *Critical Reviews™ in Oncogenesis* 13, no. 4 (2007): 303–328, https://doi.org/10.1615/critrevoncog.v13.i4.30.

25. Y. Touitou, A. Reinberg, and D. Touitou, "Association Between Light at Night, Melatonin Secretion, Sleep Deprivation, and the Internal Clock: Health Impacts and Mechanisms of Circadian Disruption," *Life Sciences* 173 (2017): 94–106, https://doi.org/10.1016/j.lfs.2017.02.008.

26. D. E. Blask, R. T. Dauchy, L. A. Sauer, J. A. Krause, and G. C. Brainard, "Growth and Fatty Acid Metabolism of Human Breast Cancer (MCF-7) Xenografts in Nude Rats: Impact of Constant Light-Induced Nocturnal Melatonin Suppression," *Breast Cancer Research and Treatment* 79, no. 3 (2003): 313–320, https://doi.org/10.1023/a:1024030518065.

27. Y. Li, S. Li, Y. Zhou, et al., "Melatonin for the Prevention and Treatment of Cancer," *Oncotarget* 8, no. 24 (2017): 39896–39921, https://doi.org/10.18632/oncotarget.16379.

28. A. Gréchez-Cassiau, B. Rayet, F. Guillaumond, M. Teboul, and F. Delaunay, "The Circadian Clock Component BMAL1 Is a Critical Regulator of p21 Expression and Hepatocyte Proliferation," *Journal of Biological Chemistry* 283, no. 8 (2008): 4535–4542, https://doi.org/10.1074/jbc.m705576200.

29. C. H. Johnson, "Circadian Clocks and Cell Division," *Cell Cycle* 9, no. 19 (2010): 3864–3873, https://doi.org/10.4161/cc.9.19.13205.

30. E. Farshadi, G. T. J. van der Horst, and I. Chaves, "Molecular Links Between the Circadian Clock and the Cell Cycle," *Journal of Molecular Biology* 432 (2020): 3515–3524, https://doi.org/10.1016/j.jmb.2020.04.003.

31. A. Gieryng, D. Pszczolkowska, K. A. Walentynowicz, W. D. Rajan, and B. Kaminska, "Immune Microenvironment of Gliomas," *Laboratory Investigation* 97, no. 5 (2017): 498–518, https://doi.org/10.1038/labinvest.2017.19.

32. T. Dickmeis, B. D. Weger, and M. Weger, "The Circadian Clock and Glucocorticoids–Interactions Across Many Time Scales," *Molecular and Cellular Endocrinology* 380, no. 1–2 (2013): 2–15, https://doi.org/10.1016/j.mce.2013.05.012.

33. A. Balsalobre, S. A. Brown, L. Marcacci, et al., "Resetting of Circadian Time in Peripheral Tissues by Glucocorticoid Signaling," *Science* 289, no. 5488 (2000): 2344–2347, https://doi.org/10.1126/science.289.5488.2344.

34. I. P. Torra, V. Tsibulsky, F. Delaunay, et al., "Circadian and Glucocorticoid Regulation of Rev-erbα Expression in Liver," *Endocrinology* 141, no. 10 (2000): 3799–3806, https://doi.org/10.1210/endo.141.10.7708.

35. G. Xiong and R. Xu, "Retinoid Orphan Nuclear Receptor Alpha (RORα) Suppresses the Epithelial-Mesenchymal Transition (EMT) by Directly Repressing Snail Transcription," *Journal of Biological Chemistry* 298, no. 7 (2022): 102059, https://doi.org/10.1016/j.jbc.2022.102059.

36. S. M. Hill, T. Frasch, Xiang Shulin, Lin Yuan, T. Duplessis, and Lulu Mao, "Molecular Mechanisms of Melatonin Anticancer Effects," *Integrative Cancer Therapies* 8, no. 4 (2009): 337–346, https://doi.org/10.1177/1534735409353332.

37. T. Fischer, M. Zmijewski, B. Zbytek, et al., "Oncostatic Effects of the Indole Melatonin and Expression of Its Cytosolic and Nuclear Receptors in Cultured Human Melanoma Cell Lines," *International Journal of Oncology* 29 (2006): 665–672, https://doi.org/10.3892/ijo.29.3.665.

38. X. Li, H. Xu, C. Xu, et al., "The Yin-Yang of DNA Damage Response: Roles in Tumorigenesis and Cellular Senescence," *International Journal of Molecular Sciences* 14, no. 2 (2013): 2431–2448, https://doi.org/10.3390/ijms14022431.

39. A. Gréchez-Cassiau, B. Rayet, F. Guillaumond, M. Teboul, and F. Delaunay, "The Circadian Clock Component BMAL1 Is a Critical Regulator of p21 Expression and Hepatocyte Proliferation," *Journal of Biological Chemistry* 283, no. 8 (2008): 4535–4542, https://doi.org/10.1074/jbc.m705576200.

40. V. Martín, F. Herrera, G. García-Santos, et al., "Involvement of Protein Kinase C in Melatonin's Oncostatic Effect in C6 Glioma Cells," *Journal of Pineal Research* 43, no. 3 (2007): 239–244, https://doi.org/10.1111/j.1600-079x.2007.00468.x.

41. S. P. Leon, R. D. Folkerth, and P. M. Black, "Microvessel Density Is a Prognostic Indicator for Patients With Astroglial Brain Tumors," *Cancer* 77, no. 2 (1996): 362–372, https://doi.org/10.1002/(sici)1097-0142(19960115)77:2<362::aid-cncr20>3.0.co;2-z.

42. S. Koyanagi, Y. Kuramoto, H. Nakagawa, et al., "A Molecular Mechanism Regulating Circadian Expression of Vascular Endothelial Growth Factor in Tumor Cells," *Cancer Research* 63 (2003): 7277–7283.

43. N. N. Guerrero-Vargas, R. Salgado-Delgado, M. C. Basualdo, et al., "Reciprocal Interaction Between the Suprachiasmatic Nucleus and the Immune System Tunes down the Inflammatory Response to Lipopolysaccharide," *Journal of Neuroimmunology* 273, no. 1–2 (2014): 22–30, https://doi.org/10.1016/j.jneuroim.2014.05.012.

44. A. González, A. González-González, C. Alonso-González, J. Menéndez-Menéndez, C. Martínez-Campa, and S. Cos, "Melatonin Inhibits Angiogenesis in SH-SY5Y Human Neuroblastoma Cells by Downregulation of VEGF," *Oncology Reports* 37, no. 4 (2017): 2433–2440, https://doi.org/10.3892/or.2017.5446.

45. M. Dai, P. Cui, M. Yu, J. Han, H. Li, and R. Xiu, "Melatonin Modulates the Expression of VEGF and HIF-1α Induced by CoCl2in Cultured Cancer Cells," *Journal of Pineal Research* 44, no. 2 (2008): 121–126, https://doi.org/10.1111/j.1600-079x.2007.00498.x.

46. R. Reiter, S. Rosales-Corral, D.-X. Tan, et al., "Melatonin, a Full-Service Anti-Cancer Agent: Inhibition of Initiation, Progression, and Metastasis," *International Journal of Molecular Sciences* 18, no. 4 (2017): 843, https://doi.org/10.3390/ijms18040843.

47. B. V. Jardim-Perassi, A. S. Arbab, L. C. Ferreira, et al., "Effect of Melatonin on Tumor Growth and Angiogenesis in Xenograft Model of Breast Cancer," *PLoS One* 9, no. 1 (2014): e85311, https://doi.org/10.1371/journal.pone.00853119.

48. K.-J. Kim, J.-S. Choi, I. Kang, K.-W. Kim, C.-H. Jeong, and J.-W. Jeong, "Melatonin Suppresses Tumor Progression by Reducing Angiogenesis Stimulated by HIF-1 in a Mouse Tumor Model," *Journal of Pineal Research* 54, no. 3 (2012): 264–270, https://doi.org/10.1111/j.1600-079x.2012.01030.x.

49. Q. Ma, R. J. Reiter, and Y. Chen, "Role of Melatonin In Controlling Angiogenesis Under Physiological and Pathological Conditions," *Angiogenesis* 23, no. 2 (2019): 91–104, https://doi.org/10.1007/s10456-019-09689-7.

50. C. Venegas, J. A. García, C. Doerrier, et al., "Analysis of the Daily Changes of Melatonin Receptors in the Rat Liver," *Journal of Pineal Research* 54, no. 3 (2012): 313–321, https://doi.org/10.1111/jpi.12019.

51. D. C. Dillon, S. E. Easley, B. B. Asch, et al., "Differential Expression of High-Affinity Melatonin Receptors (MT1) in Normal and Malignant Human Breast Tissue," *American Journal of Clinical Pathology* 118, no. 3 (2002): 451–458, https://doi.org/10.1309/1t4v-ct1g-ubjp-3ehp.

52. V. Martín, F. Herrera, P. Carrera-Gonzalez, et al., "Intracellular Signaling Pathways Involved in the Cell Growth Inhibition of Glioma Cells by Melatonin," *Cancer Research* 66, no. 2 (2006): 1081–1088, https://doi.org/10.1158/0008-5472.can-05-2354.

Supporting Information

Additional supporting information can be found online in the Supporting Information section.